Optica Applicata, Vol. XXXIII, No. 1, 2003

Light behaviour in polymer optical fibre bend – a new analysis method

MICHAŁ BORECKI

Institute of Microelectronics and Optoelectronics, Warsaw University of Technology, ul. Koszykowa 75, 00–662 Warszawa, Poland.

The paper presents light behaviour in polymer optical fibre bend, especially power transmission and near field power pattern in the fibre core. The characteristic parameters of polymer optical fibre (POF) are large core diameter and large numerical aperture. This fibre can be bent in small radius of curvature that is comparable with a fibre core radius. This way, the geometrical properties of polymer optical fibre bending geometry should not be omitted in power transmission calculations as is known for single-mode fibres. The analysis presented in this work has been done by nonlinear ray tracing technique. The novelty of this method implementation is the use of Bezier's curve for exact description of the bend and skew rays propagation analysis. The results obtained indicate that when the convergence conditions of method are met, theoretical results are in accordance with the experiment data.

Keywords: optical fibre, bend, power losses, relative transmission, rays tracing.

1. Introduction

Nowadays, we can observe the development of transmission and sensor systems based on POF. The characteristic parameters of POF are large core diameter, large numerical aperture, high flexibility and low sensitivity to the environmental influence, see Tab. 1. The values presented were assumed in further calculations.

The data show that fibre could be installed in room corners, so it can be used in a local computer network. For example, Hewlett–Packard offers commercial systems HFBR including one POF, transceiver, receiver and connectors that can transmit 1 MBd* over 34 m or 40 kBd for 145 m distance. The complete transmitting system with one fibre needs parallel to serial and serial to parallel converters with encoders. The encoders merge the data and clock into a single bitstream. This way the data in fibre will not remain in the logic 1 or 0 states for indefinite time intervals [1], which enables the high speed of detection.

*The Bd. and BPS are perhaps some of the most misused terms in the computing and telecommunications field. Many people use these terms interchangeably, though in fact they do not mean the same. The BPS is the number of bits transmitted per second. The baud rate is a measure of how many times per second a signal could change.

Table 1. Fibre parameters used in presented work.

Fibre	Core diameter [μm]	Clad	Buffer diameter [mm]	Core refraction coefficient
PFM-750-22E	750±10	chemical deposited	2.2	1.492

There are also many sensors using POF [2]–[4] formed in various shapes. The applications show that the fibre bend is sometimes desirable and sometimes unavoidable. Therefore, a method of light behaviour analysis in bent POF is needed.

The standard method based on full electric field description in large core fibre with additional complex geometry makes the internal power profile intractable [5]. Another approach that uses the beam propagation method cannot handle this case yet. The hybrid method of the ray tracing and the laws of reflection and refraction in a fibre have shown its performance [6], [7]. However, due to the assumed simplifications, the geometries of bends considered so far are fragments of a circular ring or torus. The authors of paper [6] stated that even the description of optical fibre bend by the three -dimensional structure of torus sector is insufficient due to transitory phenomena occuring between torus and direct sections of optical fibre as a result of skew radiation. It is for this reason that the Bezier curve with three-dimensional structure of fibre was used to describe the optical fibre bend in the present work.

2. Power propagation in large core optic of fibre

The fundamental idea underlying geometrical optics is to trace characteristic rays, for example, crossing the focal point of lens and parallel to optic axis of a system to obtain the formation of an image. For complex optical systems the optical ray tracing has been used. It relies on path analysis of many rays initially ordered on the basis of the law of geometrical optics. Sometimes, the initial order of rays is known as the statistical distribution. In such a case the Monte Carlo method can be used. In its standard version, many rays are traced concurrently over small time intervals, which, therefore, requires capacious memory and high speed of computer. In this paper, the vector version of Monte Carlo procedure was implemented where rays are routed separately between physical phenomena. There are many phenomena that occur along the ray traced in POF. They can be modelled deterministically or statistically as well as can be nonlinear. The present method contains such models, so it belongs to nonlinear ray tracing.

We should see that POF is used with non-coherent light source such as multimode LD or LED, and values of the POF refraction coefficients of the core and the clad are much the same, so the light polarisation effects can be omitted [8]. We assumed that the fibre bend is preceded by its straight segment in which the power distribution is stationary. This distribution is described by the near and far field patterns of power which we investigate according to procedure presented in [9].

Tab. 1. Continued

Clad refraction coefficient	Numerical aperture	Attenuation [dB/km]	Bend radius [mm]
1.419	0.46±0.02	100	20

The near field pattern was measured by processing the picture from CCD camera coupled with microscope objective. The processing consists in raster to vector conversion with 16 degrees of contour filling greyness. The white colour was assumed to correspond to the higest power density. The results obtained show that the near field pattern has constant character, as seen in Fig. 1.

The far field pattern corresponds to power angle distribution in the fibre core. It was obtained by examining the power angle profile at a distance of 10 cm from the fibre end, with the processing being based on Snell's law. This distribution was compatible with the normal one.

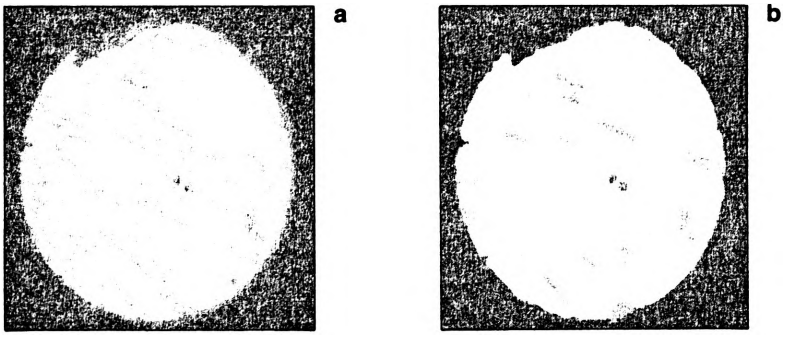

Fig. 1. Near field pattern of power in the fibre-end surface **a** – picture, **b** – vector map.

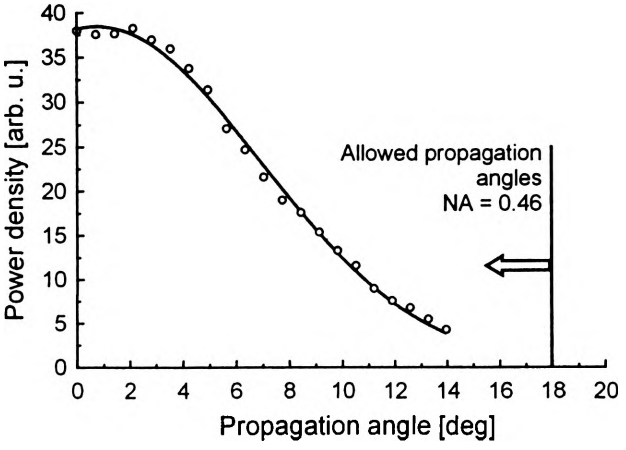

Fig. 2. Far field pattern of power in the fibre core (o data, and —— Gauss curve interpolation: mean deviation 0.7797, standard deviation 6.13457, area under curve 591.51).

The power distributions from Figs. 1 and 2 were assumed as initial conditions for further discussion and calculations.

Next, we can see that power attenuation in a linear segment of the fibre depends on surface scattering and absorption losses. To describe quantitatively the magnitude of such losses, the exponential attenuation coefficient is generally used. The light intensity (power per area) at any point along the length of straight fibre is described as follows:

$$I(y) = I(0)\exp(-\rho_{sa}y) \tag{1}$$

where $I(y)$ is the light intensity as a function of y position along the fibre, ρ_{sa} is the attenuation coefficient due to scattering and absorption losses. In our analysis the maximum lengths of fibre segments are relatively small. For example, the length of half of circular fibre bend with radius of 30 mm meets mentioned losses of 9.42×10^{-3} dB. Therefore, such an attenuation could be neglected in fibre bend ($\rho_{sa} = 0$). So, it has been assumed that the power of analysed ray is constant between reflections and reflection planes are linear. Thus, a single ray propagating in three -dimensional space of an optical fibre between reflections can be described with the use of three parametric equations:

$$\begin{aligned} x &= x_s + \tau x_k, \\ y &= y_s + \tau y_k, \\ z &= z_s + \tau z_k \end{aligned} \tag{2}$$

where: x_k, y_k, z_k determine the directional vector coefficients, x_S, y_S and z_S are the starting point co-ordinates, τ is the parameter, because the ray power is constant. The plain segment of fibre can be geometrically described as a cylinder

$$x^2 + z^2 = r^2 \tag{3}$$

where r is the fibre core radius.

The ray reflection in fibre is the most interesting case. It is presented in Fig. 3. The reflection occurs at a point, where parameter τ equals

$$\tau = \frac{\sqrt{r^2(x_k^2 + z_k^2) - x_k^2 z_s^2 + x_s z_k(2x_k z_s - x_s z_k)} + x_k x_s + z_k z_s}{x_k^2 + z_k^2}. \tag{4}$$

The ray directional vector after reflection can be determined from:

$$\begin{aligned} x_k &= \frac{2}{r^2}[x_r^2(x_p - x_r) + x_r z_r(z_p - z_r)] + x_r - x_p, \\ y_k &= y_r - y_p, \\ z_k &= \frac{2}{r^2}[x_r z_r(x_p - x_r) + z_r^2(z_p - z_r)] + z_r - z_p \end{aligned} \tag{5}$$

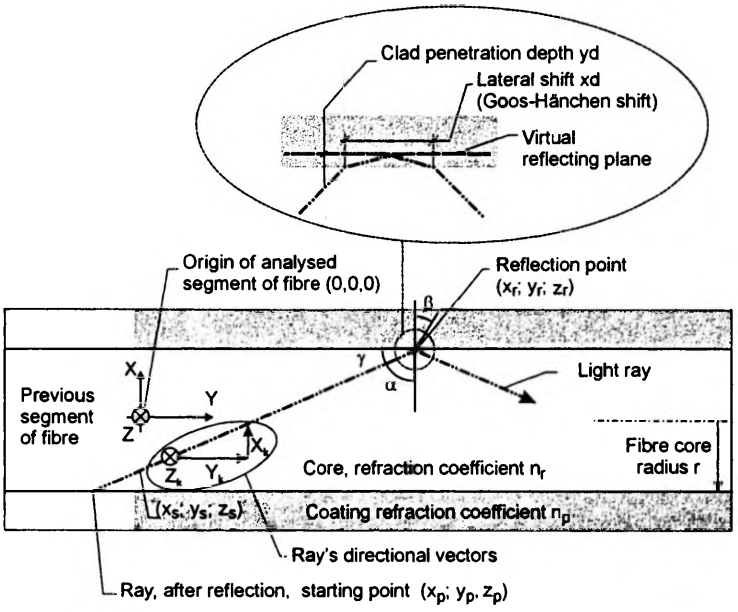

Fig. 3. Ray reflection in the optical fibre, two-dimensional projection.

where x_r, y_r and z_r are reflection point co-ordinates; x_p, y_p, z_p are previous reflection point co-ordinates. The angle of ray incidence is

$$\alpha = \arccos\left(\frac{\left|-x_p x_r + x_r^2 - z_p z_r + z_r^2\right|}{\sqrt{(x_r - x_p)^2 + (y_r - y_p)^2 + (z_r - z_p)^2} \times \sqrt{x_r^2 + z_r^2}}\right) \tag{6}$$

and when

$$\alpha > \alpha_c = \arcsin\frac{n_p}{n_r} \tag{7}$$

the ray reflects without losses. In other cases, the power losses are defined by power reflection Fresnel coefficient R which for non polarised light is as follows:

$$R = \frac{1}{2}\left[\frac{\sin^2(\alpha-\beta)}{\sin^2(\alpha+\beta)} + \frac{\tan^2(\alpha-\beta)}{\tan^2(\alpha+\beta)}\right]. \tag{8}$$

At reflection point the amplitude of refracting ray decays exponentially in the clad with the distance from interface of the core and the clad [8]. This amplitude function can be written as

$$A(y_d) \div \exp(-\kappa \times y_d) \tag{9}$$

where: y_d is the penetration depth, coefficient κ is defined as

$$\kappa = \frac{2\pi}{\lambda}\sqrt{\frac{\sin^2(\alpha)}{(n_p/n_r)^2} - 1} \tag{10}$$

where λ is the ray wavelength in the clad; we assumed for further calculations $\lambda = 635$ nm. This results in a lateral shift of the reflected ray, known as the Goos –Hänchen shift. The Kapany–Burke model describes the ray path by introducing virtual reflection plane. According to it, the ray penetration depth equals the coefficient κ converse. The ray penetration depth reaches maximum when angle of incidence approaches the critical one and decreases very fast when the incidence angle increase. The minimum value of penetration depth is recorded for incidence angle tending to zero, which in our case equals 311 nm. For power transmission it is important to know what amount of power is necessary to penetrate the clad deeply. This question can be answered by solving the system of Eqs. (9), (10) and considering the power far field distribution, given here by

$$s(\gamma) = \frac{1}{\text{std}\sqrt{2\pi}}\exp\left[-\frac{1}{2}\left(\frac{\gamma - m}{\text{std}}\right)^2\right],$$

$$\gamma = \frac{\pi}{2} - \alpha \tag{11}$$

where: γ is the propagation angle, standard deviation (std) is 6.13°, mean $m = 0$, angle of incidence $\alpha \in (\alpha_c; 90°)$, see Fig. 4.

The results show that 75% of power penetrates clad to a depth of less than 1.3 μm, 99% of power penetrates to not more than 2.9 μm. On the other hand, the core diameter of the fibre analysed varies ±10 μm. Therefore, the power penetration depth is significantly below the core diameter variation. Consequently, according to [10], the Goos–Hänchen shift can be omitted in the case being analysed.

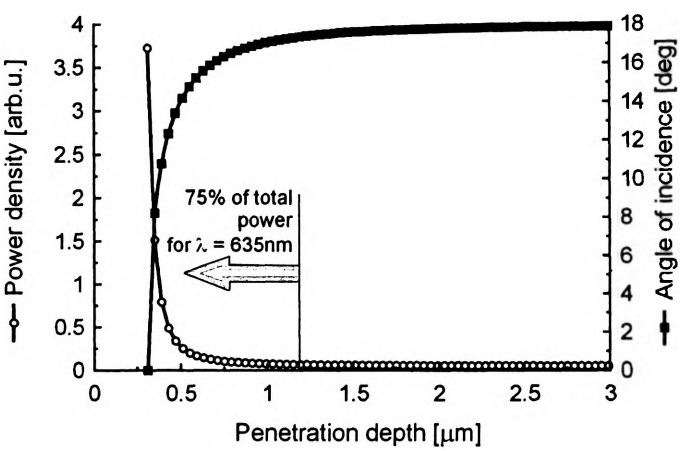

Fig. 4. Power *vs.* clad penetration.

Taking into accound the above facts, we conclude that the precision of the fibre bend geometry description is the most important factor in analysis of power losses in fibre bend.

3. Optical fibre bend

In practice, you can rarely find implementations of optical fibre that would consist of straight fibre sections only. Optical fibre path is typically described as a composition of line sections connected with circle sectors; therefore, the representation of fibre geometry is not precise. It was mentioned [6] that the most exact description of it should be used in power transmission calculations. Therefore, when describing the bent sector of an optical fibre we use the Bezier curve of the third degree

$$\begin{cases} y(t) = y_0(1-t)^3 + y_1 3t(1-t)^2 + y_2 3t^2(1-t) + y_3 t^3 \\ x(t) = x_0(1-t)^3 + x_1 3t(1-t)^2 + x_2 3t^2(1-t) + x_3 t^3 \end{cases} \tag{12}$$

where: $(x_0; y_0)$ is the starting point of the curve, $(x_1; y_1)$, $(x_2; y_2)$ are control points, $(x_3; y_3)$ is the end point, $t \in \langle 0; 1 \rangle$ is a parameter. In this work, the curve described by Eqs. (12) represents the route of the local symmetry axis of fibre core. The bend was described in a discrete manner, as a series of angle connected cylinders. The radius of cylinder basis equals the radius of fibre core. The length of its generating line depends on the level of digitisation and the shape of the curve because Bezier's curve condense

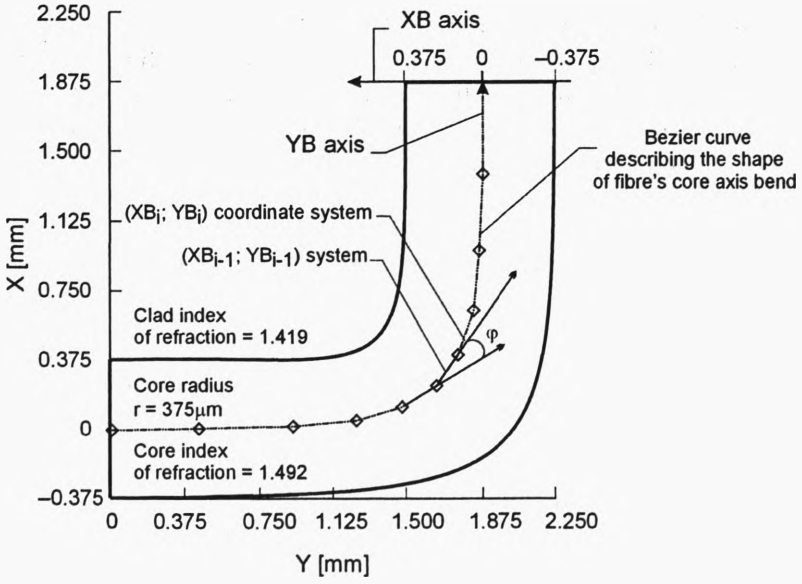

Fig. 5. Bend of optical fibre described by Bezier curve with the (*XB*; *YB*) co-ordinate system.

points $(x(t); y(t))$ in the areas of higher geometry changes. The sample of bent optical fibre geometry is shown in Fig. 5. The rhombuses on the core symmetry axis represent the points of fibre division.

After introducting a new co-ordinate system $(XB; YB)$ in which XB axis is a "straightened" axis of the optical fibre and YB axis is perpendicular to XB axis, a relatively simple method for analysing the ray path in optical fibre bent has been obtained. The aim is to assess its path in straight sections of the optical fibre. Then, the ray directional vector changes at points of the division of fibre sections. For the following two sections with slope φ the relation between co-ordinates in systems $(XB_i; YB_i)$ and $(XB_{i-1}; YB_{i-1})$ is:

$$x_i = x_{i-1}\cos\varphi - y_{i-1}\sin\varphi,$$
$$y_i = y_{i-1}\cos\varphi - x_{i-1}\sin\varphi. \tag{13}$$

Therefore, Eqs. (2) change with ray crossing the next cylinder

$$x = x_s + \tau(x_k\cos\varphi - y_k\sin\varphi),$$
$$y = y_s + \tau(y_k\cos\varphi - x_k\sin\varphi),$$
$$z = z_s + \tau z_k \tag{14}$$

where: x_s, y_s, z_s – points of ray on cylinder-end surface; x_k, y_k, z_k – directional vector in preceding cylinder.

4. Nonlinear ray tracing simulation according to Monte Carlo scheme

The beginning of Monte Carlo scheme is random generation of input rays according to known power distributions. The random numbers generator is used for this purpose. Its quality is defined by the period and distribution parameters. In the environment used (MathCad), the period of the generator is 4.68×10^8. The distribution parameters are presented in Tab. 2. On such basis we can assume that generator parameters are satisfactory.

Table 2. Average value and variance test results for random number generator with the range (0;1) and uniform distribution built into MathCad.

No. of rays	Average value	Variance of the value	Error of the average	Error of the variance
10000	0.502823	0.083236	0.565	–0.116
100000	0.500304	0.083072	0.061	–0.314

Note that the number of independent simulations is limited in advance by random generator period rising to 2/3 power and divided by the number of random generator runs in one simulation.

4.1. Ray generation

To describe initial ray co-ordinate $(x_s; y_s; z_s)$ a pair of numbers $(x_1; z_1)$ were generated from square circumscribed circle of fibre core. The co-ordinate that was out of the core area was omitted. The y_s co-ordinate was assumed 0. Next, directional vector on X–Z surface was constructed by generating a pair of numbers $(x_2; z_2)$. Then the slope γ of ray to core axis was generated. This way, for the ray in three-dimensional space generation that is described by 6 numbers we use statistically 6.09 generator runs. Therefore, the number of rays in one simulation is limited here to 9.88×10^4. It has been shown that for 10×10^3 rays propagated by a torus segment it is enough to calculate transmission with one percent precision [6].

The arbitrary power field distribution can be generated using the procedure presented. The near power field is defined here by distribution of $(x_1; z_1)_i$ and $(x_2; z_2)_i$. When these points have uniform distribution, the uniform near power field is simulated. The Gaussian near field is simulated when $(x_1; z_1)_i$ have uniform distribution and $(x_2; z_2)_i$ have two-dimensional Gaussian distribution, where mean values are equal to the co-ordinate of fibre core axis. In this case, the balance between the number of meridional and skew rays is possible by standard deviation changing. The qualitative dependence can be described as the less standard deviation from the number of meridional rays is greater. In this way, the smallest ray distance from core axis at fibre core intersection could be assumed as a measure of skewness, see Fig. 6.

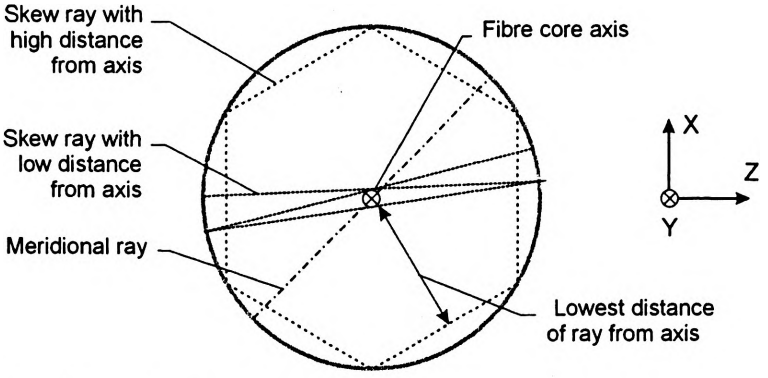

Fig. 6. Kinds of rays at fibre core intersection.

The far field pattern is defined here by the generated rays slope γ_i distribution. In the case analysed the near power field is uniform and the far field is Gaussian. It means that $(x_1; z_1)_i$ and $(x_2; z_2)_i$ have uniform distribution and γ_i has Gaussian distribution here.

4.2. Calculation tolerance

To check the correctness of the method and assess its precision the relative transmission and output power distribution calculations were done, considering the

worst case. Since it is known that calculations are more convergent and more precise when geometry of the system is simpler [11], the test was done for half a circle fibre bend with 20 mm radius of curvature. This curvature radius has the lowest permissible value for long time bending. For simulation purposes the half circle was approximated with the Bezier curve consisting of 1000 sections. The calculated control points of the curve were (–20; 0), (–20; 26.37), (20; 26.37) and (20; 0). The mean square error of circle shape approximation was 0.16% of its radius, and maximum error was 1.39%. As we can see, this approximation meets accuracy of the fibre core position in the coat. The simulations, with a change in the number of curve sections, show that precision in shape description is one of the most important factors of this simulation technique. Therefore, it is very important to use as accurate shape description as in real cases.

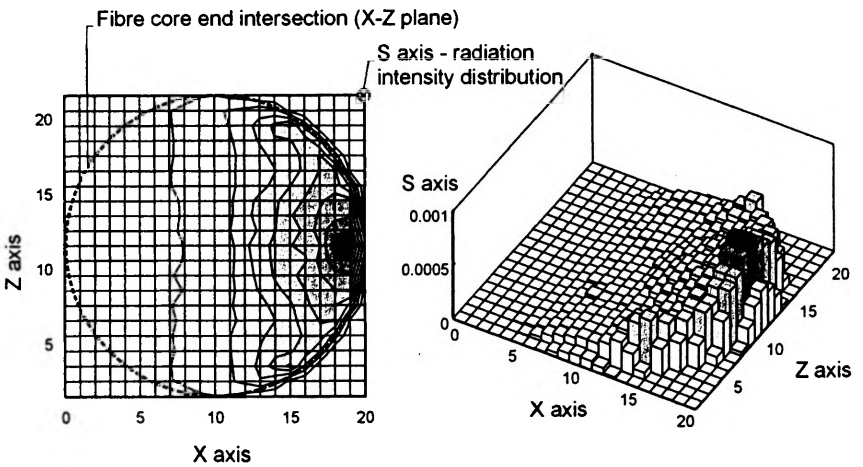

Fig. 7. Calculated near field pattern for 20×20 element mesh in top and perspective views.

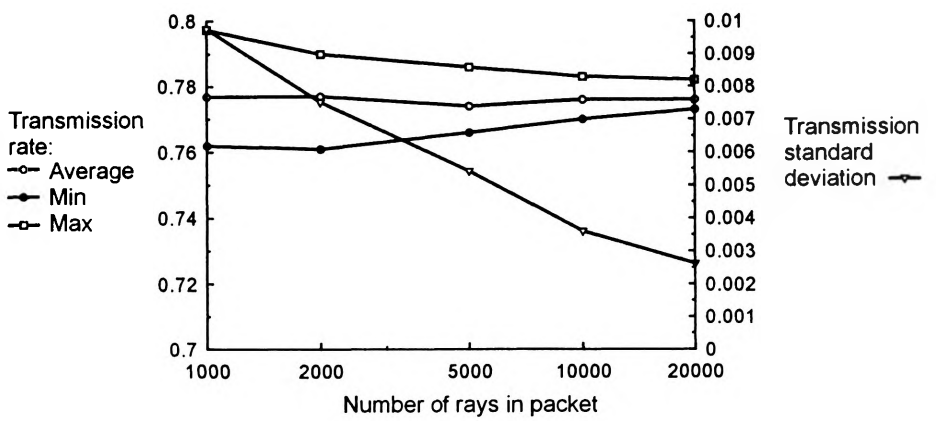

Fig. 8. Convergence of relative transmission rates for radiation passing half a ring bent fibre *vs.* the number of rays in a packet.

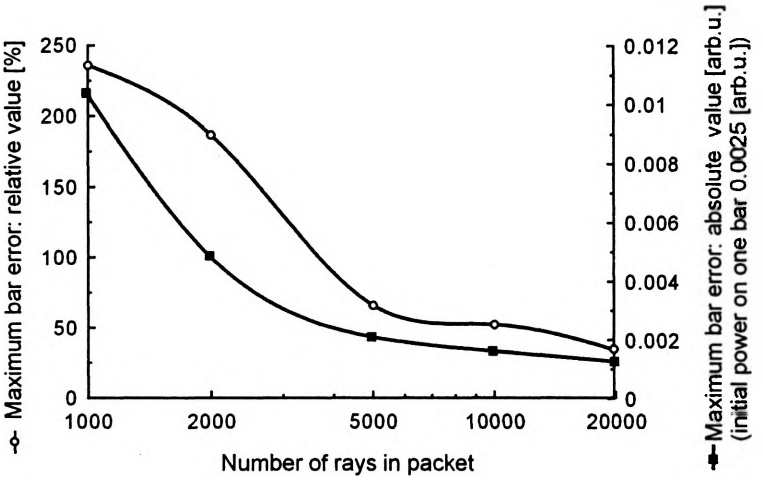

Fig. 9. Convergence of near field calculation for radiation passing half a ring bent fibre *vs.* the number of rays in a packet.

With such parameters the power transmission calculation tests have been made. First, the relative transmission rate and the near field pattern for maximum permissible number of rays have been calculated. The relative power transmission rate equals 0.776. The near field pattern has been calculated for 20×20 element mesh and is presented in Fig. 7. As we can see, the shape of the near field pattern is quite well defined here.

The above results have been assumed as accurate for the simulation convergence tests. The tests have been carried out for a step-by-step increasing number of rays in a packet (10^3, 2×10^3, 5×10^3, 10^4, 2×10^4). The result for twelve statistically independent simulation runs for each packet is presented in Figs. 8 and 9.

The errors of calculated power transmission and near field pattern appear to decrease with the number of rays in a pocket. Furthermore, according to [6] for 10 thousand rays in packet the error of power transmission simulation stabilises at the level of one per cent (in our case, 1.67%). The calculated near field pattern relative error is quite big but it has small absolute values compared with the value of power transmission.

5. Experimental verification

The method presented has been experimentally verified for relative power transmission rate and relative near field pattern cases. First, data of relative transmission rate has been obtained in direct measurements for the fibre configurations shown in Fig. 10. The results of this experiment and the calculated transmission relative rate are put together in Fig. 11.

These characteristics show that the method allows assessment of the relative transmission rates. The critical curvature radius can be determined precisely, which

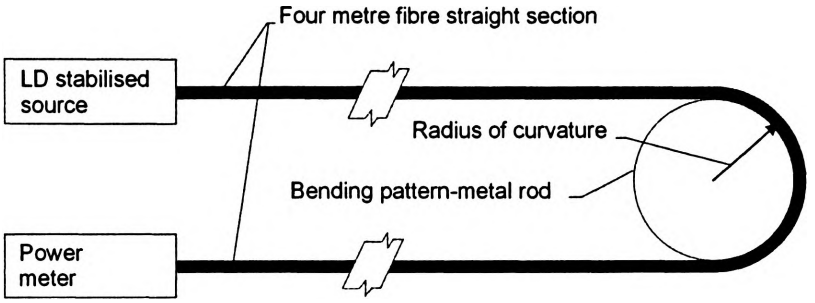

Fig. 10. Direct measurement of transmission for half a ring fibre section.

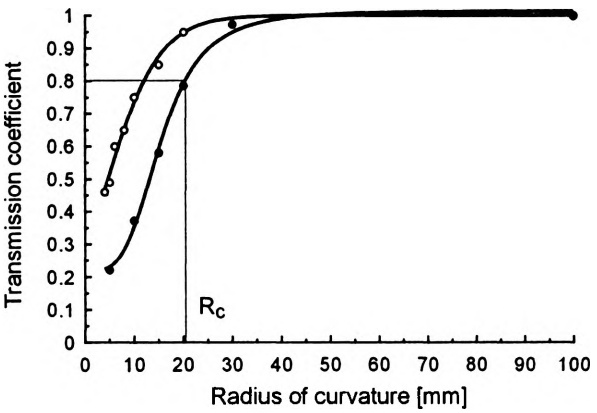

Fig. 11. Relative transmission rates for radiation passing half a ring bent fibre *vs.* radius of curvature (–o– experimental data, –•– calculated data).

for the fibre analysed equals 20 mm. This value agrees with the one indicated by producer as allowable bending radius of curvature and corresponds to the experimental results, too. The measured transmission rate differs insignificantly from the calculated ones for a region of large losses. This can be caused by the presence of clad radiation in the real experiment that is not taken into account in the elaborated model.

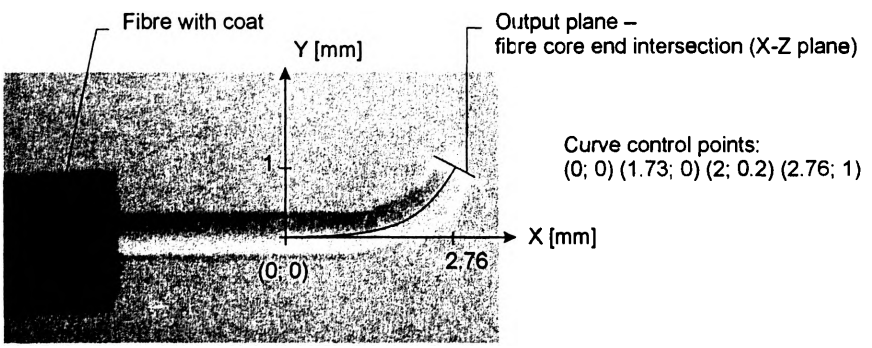

Fig. 12. Fibre bend with approximation of core shape by the Bezier curve.

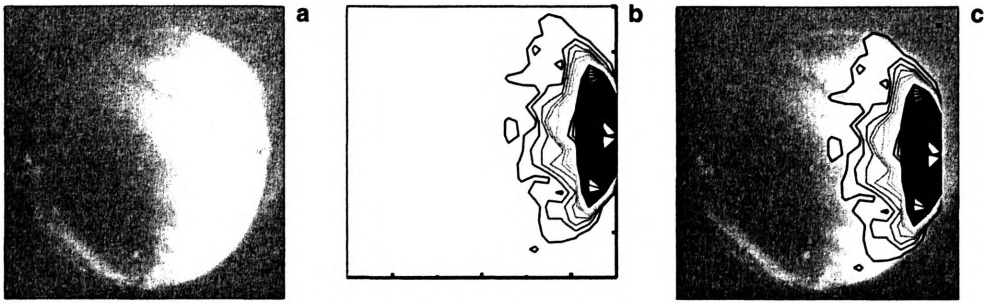

Fig. 13. Near field patterns for fibre geometry presented in Fig. 12: **a** – experimental, **b** – calculated, **c** – merge of calculated and experimental results.

The near field pattern has been investigated for the case of low curvature radius. The fibre bending has been formed on cast profile. The fibre was without a coat in this experiment, so the curve of core axis could be precisely fit, as presented in Fig. 12.

For such a geometry the near field pattern has been calculated and measured. The results presented in Fig. 13 show that there is at least a quality agreement between these fields. During experiments the clad radiation has been observed. The effects it exerts on the near field pattern have been represented by background level in the whole fibre end plane and by increasing and broadening the radiation area. The clad radiation has decreased when the fibre bend was immersed in absorbing medium.

6. Summary

The method proposed allows proper assessment of critical curvature radius of multimode optical fibre bend and relative power transmission rate by the bend fibre represented by the Bezier curve of the third degree. This method also enable determination of near field pattern in the bend fibre. These facts were proved experimentally. For those reasons the method is suitable for the design of multimode optical fibre components. It is possible to determine power transmission rate and near field pattern in complex geometry components by introducing the Bezier curve of higher order. The method can be made more precise by introducing clad rays into analysis.

References

[1] Agilent Technologies, *Fiber Optic Components CookBook*, Agilent Technologies web library: www.semiconductor. agilent.com (1999).
[2] Borecki M., Kruszewski J., Bebowska M., Opto-electronics Rev. **7** (1999), 203.
[3] Borecki M. Kruszewski J., Kopczyski K., Opt. Appl. **30** (2000), 141.
[4] Hadjiloucas S., Irvine J., Keating D.A., Meas. Sci Technol. **11** (2000), 1.
[5] Kuhn A., Blewett I.J., Hand D.P., French P., Richmond M., Jones J.D.C., Opt. Lasers Eng. **34** (2000), 273.

[6] ARRUE J., ZUBIA J., FUSTER G., KALYMNIOS D., IEE Proc.: Optoelectron. **145** (1998), 313.
[7] BECK TH., RENG N., WEBER H., Opt. Lasers Eng. **34** (2000), 255.
[8] RAYSS J., SUDOLSKI G., Opto-electronics Rev. **8** (2000), 129.
[9] *Hitachi Optodevice Data Book*, [Ed.] Technical Document Center Hitachi Microcomputer System, Ltd., Hitachi, Tokyo, August 1995.
[10] SENIOR J.M., *Optical Fiber Communications – Principles and Practice*, Prentice Hall, Second edition, 1992.
[11] BORECKI M., [In] *V Scientific Conference Optoelectronic and Electronic Sensors*, Vol. 1, Jurata, Poland 1998, p. 135 (in Polish).

Received March 14, 2002
in revised form July 9, 2002